Diamond & Related Materials 130 (2022) 109431

Contents lists available at ScienceDirect

Diamond & Related Materials

journal homepage: www.elsevier.com/locate/diamond

Capture of novel sp^3 hybridized Z-BN by compressing boron nitride nanotubes with small diameter

Ying Zhang [a], Shuang Liu [a], Zhen Yao [a], Jiajun Dong [a], Bo Liu [a], Ran Liu [a,*], Mingrun Du [b], Peng Wang [a], Quanjun Li [a], Thomas Wågberg [c], Hamid Reza Barzegar [c], Alex Zettl [d], Mingguang Yao [a,*], Bingbing Liu [a,*]

[a] State Key Laboratory of Superhard Materials, College of Physics, Jilin University, Changchun 130012, China
[b] Civil Aviation University of China, College of Science, Tianjin 300300, China
[c] Department of Physics, Umeå University, 90187 Umeå, Sweden
[d] Department of Physics, University of California at Berkeley, Materials Sciences Division, Lawrence Berkeley National Laboratory, Kavli Energy Nano Science Institute at the University of California at Berkeley, Lawrence Berkeley National Laboratory, Berkeley, CA 94720, USA

ARTICLE INFO

Keywords:
High pressure
Boron nitride nanotubes (BNNTs)
Sp^3 hybridized materials
Stacking sequence

ABSTRACT

Experimental synthesis of new sp^3 hybridized carbon/boron nitride structures remains challenging despite that numerous sp^3 structures have been proposed in theory. Here, we showed that compressed multi-walled boron nitride nanotubes (MWBNNTs) and boron nitride peapods (C_{60}@BNNTs) with small diameters could transform into a new sp^3 hybridized boron nitride allotrope (*Z*-BN). This strategy is considered from the topological transition point of view in boron nitride nanotubes upon compression. Due to the increased curvature in compressed small-diameter MWBNNTs, the uncommon 4- and 8-membered rings in *Z*-BN could be more favorably formed. And the irreversible tube collapse is proved to be a critical factor for the capture of the formed *Z*-BN, because of the competition between the resilience of tube before collapse and the stress limitation for the lattice stabilization of Z-BN upon decompression. In this case, Z-BN starts to form above 19.0 GPa, which is fully reversible below 45 GPa and finally becomes quenchable at 93.5 GPa. This collapse-induced capture of the high-pressure phase could also be extended to other tubular materials for quenching novel sp^3 structures.

1. Introduction

Both B and N atoms can form *sp*, sp^2, and sp^3 hybridized bonding and thus could form various boron nitride (BN) allotropes due to the flexible bonding ability, which is similar to that of carbon. Particularly, due to the strong sp^3-bonded framework, cubic boron nitride (c-BN) and diamond are two well-known superhard materials that have been widely used as abrasive and cutting tools for hard substances such as stones, glasses, and ceramics [1–6]. Compared with diamond, c-BN possesses a wider band gap, and better thermal and chemical stability, thus exhibiting advantages for advanced electronic devices, coating material, cutting ferrous and carbide-forming hard substances [7,8]. Because of these advantages, sp^3-boron nitride allotropes have attracted intensive attention. Up to now, plenty of sp^3 BN allotropes have been theoretically predicted [9–14], but only c-BN and wurtzite BN (w-BN) have been synthesized experimentally [8,15–20]. Among these studies, high pressure (HP)/high pressure and high temperature (HPHT) is an efficient technique to search for sp^3-BN allotropes, in which the stacking sequences of BN layers are critical for the new structure formation. Despite various BN precursors with different structures, such as boron nitride nanotubes (BNNTs) and amorphous BN have been studied for new sp^3 BN structures, but the obtained stable phases remain w-BN structure or c-BN [17,20–22]. Therefore, experimental synthesis of new sp^3 hybridized boron nitride structures that could be stable at ambient conditions remains challenging.

In fact, the stacking sequence of BN layers in the starting precursor plays a crucial role in a phase transition. One example is the formation of c-BN through intralayer buckling and interlayer bonding of ABC-stacking BN (r-BN) under pressure [23], while w-BN could be formed from compressing bulk h-BN with AA′-stacking [17,24]. In contrast to planar h-BN, a nanotube can be considered as a rolled-up h-BN sheet with a hollow cylindrical shape. The nested construction composed of

* Corresponding authors.
E-mail addresses: liuran@jlu.edu.cn (R. Liu), yaomg@jlu.edu.cn (M. Yao), liubb@jlu.edu.cn (B. Liu).

https://doi.org/10.1016/j.diamond.2022.109431
Received 29 July 2022; Received in revised form 5 September 2022; Accepted 3 October 2022
Available online 7 October 2022

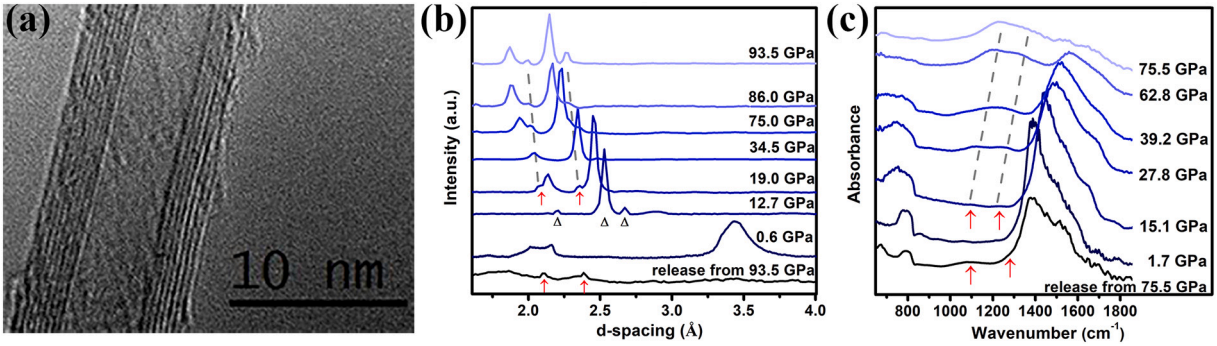

Fig. 1. (a) TEM image of a starting multi-walled boron nitride nanotube. (b) High-pressure XRD patterns (using argon as the pressure transmitting medium). The obvious peaks marked with triangles are attributed to solidified argon under pressure. (c) High-pressure IR spectra of MWBNNTs (the background has been carefully subtracted).

coaxial tubes with different diameters of multi-walled tubes could show tunable stacking sequences and should be more stable than the planar layered h-BN that usually shows interlayer sliding upon compression. Despite that new sp^3 BN structures have been theoretically predicted by compressing BNNTs with different chirality and diameters and the emerging structures are nanotube diameter dependent [9–11,25,26], experimental progress is still very limited, and only w-BN and c-BN have been observed in compressed BNNTs. A recent high-pressure study showed that MWBNNTs transformed into various sp^2-hybridized tube with different morphologies [27]. Note that the previous studies are mainly working on large MWBNNTs with diameters from 50 to 100 nm, in which the curvature could be ignored and the stacking sequences are in large equivalent to bulk h-BN. In contrast, BNNTs with smaller diameters should have stronger curvature and distinct stacking sequences, which are likely more prone to transform into novel sp^3 hybridized BN materials under high pressure.

Here, we report a new sp^3 hybridized BN with orthorhombic structure by compressing MWBNNTs with diameters ranging from 2 to 5 nm and boron nitride peapods (C_{60}@BNNTs). The different stacking sequences of curved tubes and spherical C_{60}s contribute to the observed formation of *Z*-BN instead of the formation of cubic or wurtzite structure, which is commonly observed by compressing hexagonal BN. Besides, it is found that irreversible tube collapse is a critical factor for the quenching of the formed *Z*-BN, because of the competition between the resilience of tube before collapse and the stress limitation for the lattice stabilization of Z-BN upon decompression. This phenomenon could also be extended to other tubular materials for synthesizing and quenching novel sp^3 structures.

2. Experimental and computational method

BNNTs, with inner diameters ranging from 2 to 5 nm (5–10 walled), were synthesized using the extended pressure inductively coupled plasma method [28]. The as-grown BNNTs were acid-treated first and further annealed at 800 °C in air for 1 h to remove possible impurities from the sample and open the closed end of the tubes [29]. The BNNTs were mixed with coronene and C_{60} (99.9 %; MER Corporation) and sealed in a quartz ampule (half-inch diameter) at 105 Torr. The quartz ampule is placed in an oven at 630 °C for 5 days. The C_{60}-filled BNNTs were dispersed in toluene to dissolve the free C_{60} molecules. The sample was then collected by filtration, using a PTFE filter with a pore size of 0.45 μm. Thereafter the sample was collected from the filter for further examination. High-pressure experiments were performed in a Mao-Bell type diamond anvil cell (DAC) at room temperature. Samples were loaded into an 80 μm diameter hole drilled in Rhenium gaskets. Two type-IIa diamonds with 0.2 mm culets were installed in the DAC for infrared (IR) spectroscopy measurements. KBr was used as a pressure transmitting medium. Small ruby balls were incorporated with the sample for pressure calibration by measurements of the shift of the fluorescence line. IR measurements were carried out using a Bruker spectrometer. *In situ* high-pressure X-ray diffraction (XRD) experiments were performed at the Shanghai Synchrotron Facility at ambient temperature ($\lambda = 0.61992$ Å). A JEOL (JEM-2200FS) instrument with an accelerating voltage of 200 kV is employed for transmission electron microscopy (TEM), selected area electron diffraction (SAED), and electron energy loss spectroscopy (EELS) analysis. Calculations were performed based on the density functional theory (DFT) *via* the Vienna *ab initio* simulation package (VASP) using plane-wave basis set. The Perdew-Burke-Ernzerhof (PBE) within generalized gradient approximation (GGA) was adopted to describe the exchange correlation functional. Full geometry optimization was performed for both the lattice and the atomic positions. The cutoff energy of 520 eV and Monkhorst-Pack *k*-meshes (*k*-points grid 0.03 $Å^{-1}$) were used in all calculations. The convergence criterion of energy was 10^{-4} eV for each structural relaxation. IR spectrum is calculated by the CASTEP code in the Materials Studio package.

3. Results and discussions

Fig. 1a shows a high-resolution transmission electron microscopy (HRTEM) image of MWBNNT with 8 walls and an inner diameter of approximately 5 nm. Overall the nanotubes in the probed sample were estimated to have inner diameters between 2 and 6 nm with 2 to 10 walls and not bundled. The structural transformations of MWBNNTs monitored by *in situ* high-pressure XRD up to 93.5 GPa are shown in Fig. 1b. The diffraction pattern at 0.6 GPa can be indexed by a hexagonal structure of BN (h-BN, ICSD card (01-085-1068)). Upon compression up to 12.7 GPa, the three peaks assigned to the hexagonal structure almost disappeared, and instead, two new diffracted peaks at 2.09 Å and 2.38 Å appeared above 19.0 GPa. These two peaks cannot be assigned to the commonly observed w-BN structure [30,31], but instead indicate the formation of a new structure. The intensities of these two diffraction peaks grow gradually as pressure increases and the new phase becomes dominating at 93.5 GPa. Note that no diffraction peaks for h-BN can be observed in the released sample, indicating the high-pressure phase was successfully quenched to ambient conditions.

High-pressure FTIR measurement up to 75.5 GPa has been further carried out on the sample (Fig. 1c) to study this structural transition. The IR spectrum for MWBNNTs at 1.7 GPa shows two major IR bands at 787 and 1391 cm^{-1}, which are characteristic modes of hexagonal BN with symmetries of A_{2u} and E_{1u}, respectively. The A_{2u} mode corresponds to the B—N stretch perpendicular to the tube axis and the E_{1u} mode corresponds to the B—N stretch parallel to the tube axis [17,32]. As pressure increases, their intensities present a global attenuation, and the E_{1u} band shows a normal blue shift, whereas the A_{2u} band exhibits a redshift which has been assigned to the dynamical buckling of the hexagonal

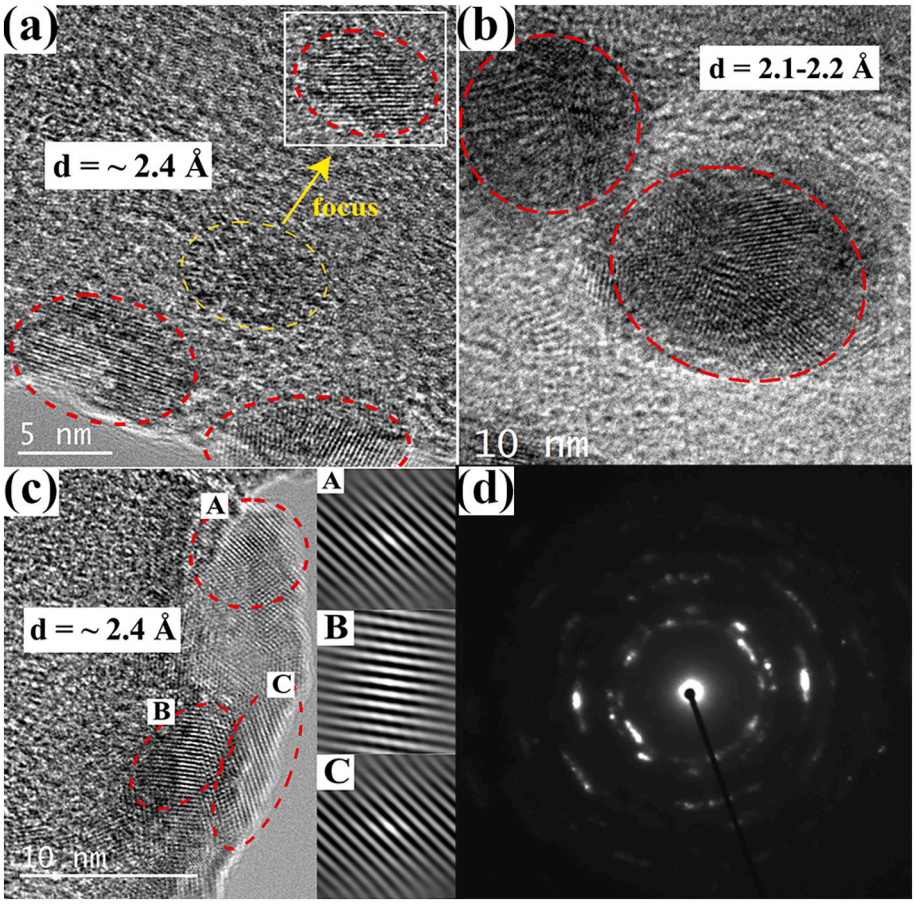

Fig. 2. (a-c) HRTEM images on the sample released from 95 GPa. The corresponding inverse fast Fourier transformation (IFFT) images are shown as insets (A, B, and C). (d) Selected area electron diffraction (SAED) pattern of the sample released from 95 GPa.

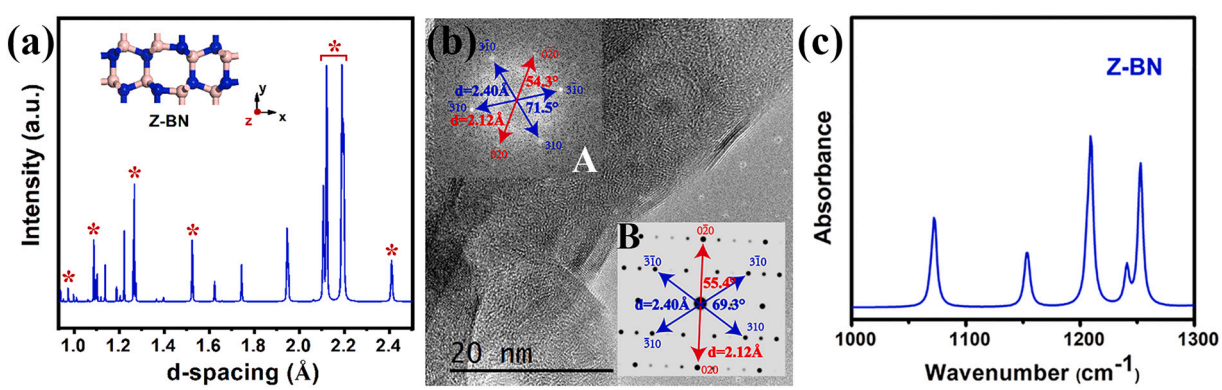

Fig. 3. (a) Calculated XRD pattern of *Z*-BN at 0 GPa. The diffraction patterns marked with red asterisks were observed in the selected area electron diffraction (SAED) pattern of the released sample in Fig. 2d. (b) Fast Fourier transform (FFT) pattern of the sample released from 95 GPa (inset A) and calculated diffraction pattern of Z-BN (inset B) with unit cell parameters a = 8.890 Å, b = 4.290 Å, c = 2.550 Å and α = β = γ = 90°. (c) The calculated IR spectrum of Z-BN.

layers [33]. At 22.3 GPa, two broad peaks at 1082 and 1214 cm^{-1} emerged, which is different from the characteristic peak of 1125 cm^{-1} for w-BN in the previous study [17]. The intensities of these two new peaks increase gradually upon further compression and become dominant at 75.5 GPa. When the pressure was released, the A_{2u} and E_{1u} bands of h-BN gained their intensity back, meanwhile, the broadband at ~1095 cm^{-1} still exists while the peak above 1200 cm^{-1} is mainly hidden in the envelope of the E_{1u} mode of h-BN. The two broad IR modes at 1082 and 1214 cm^{-1} are not from w-BN and c-BN, further supporting that new structure was created in our experiment. In addition, this new structure can be quenched to ambient pressure from 93.5 GPa, while the h-BN is likely at least partly recovered when decompressed from 75.5 GPa.

The structures of the recovered samples have been carefully studied by HRTEM (Fig. 2a-c). When released from 95 GPa, no nanotubes can be observed, and instead, some nanocrystalline particles with diameters of around 10 nm surrounded by some amorphous structure can be observed. The corresponding d-spacings are approximately 2.1–2.2 Å, and 2.40 Å, which are in good agreement with the observed diffraction peaks at 19.0 GPa in our *in situ* XRD measurements (Fig. 1b). Furthermore, the selected area electron diffraction pattern (Fig. 2d) of the released sample shows several Miller planes with d-spacings of ~2.46,

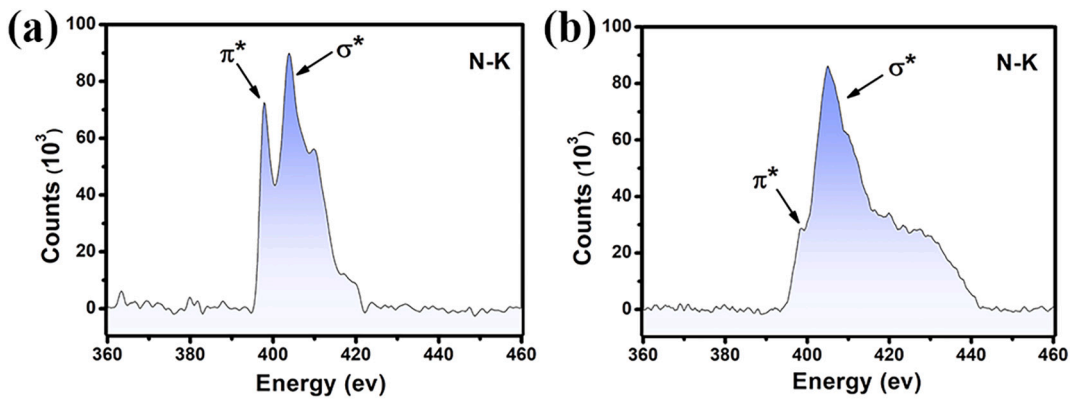

Fig. 4. N—K edge electron energy loss spectra of (a) the original BNNTs and (b) the sample released from 95 GPa.

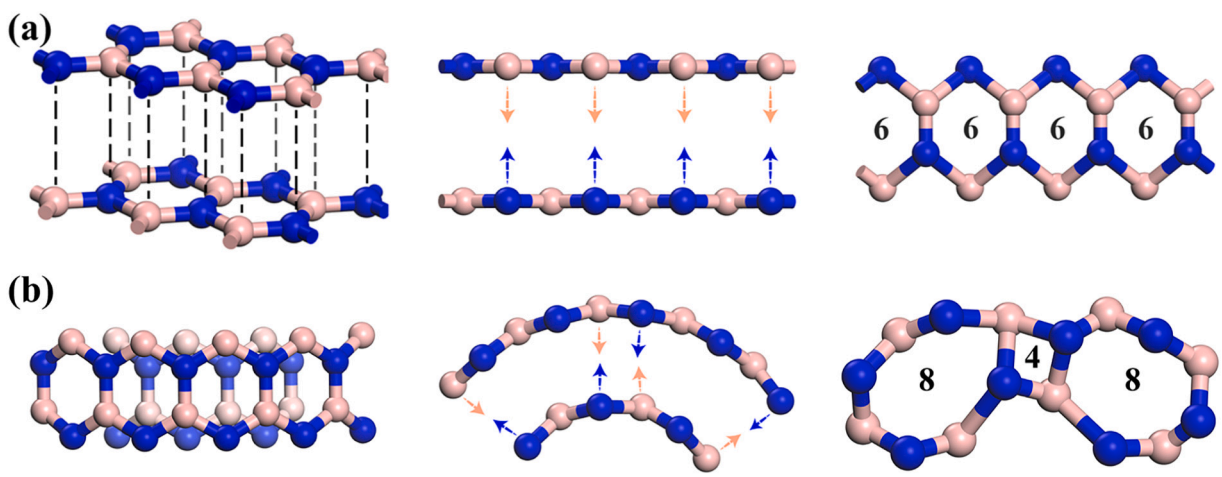

Fig. 5. Proposed transformation pathways of (a) AA′ stacking h-BN and (b) AB stacking BNNT fragment under cold compression. The pink and blue balls represent boron and nitrogen, respectively.

2.1–2.2, 1.52, 1.25, 1.07, and 0.97 Å, which are consistent with the calculated diffraction patterns of *Z*-BN at 0 GPa (marked with red asterisks in Fig. 3a). In addition, the fast Fourier transform (FFT) pattern (upper inset in Fig. 3b) shows two interplanar crystal spacings of 2.12 Å and 2.40 Å, which correspond to the d-spacings of (020) and (310) in *Z*-BN. The cross angles between $(0\bar{2}0)$ and $(3\bar{1}0)$ planes, $(3\bar{1}0)$ and (310) planes are 54.3° and 71.5°, which are also consistent with the interplanar angles calculated for *Z*-BN (inset B in Fig. 3b). Further theoretical support is gained from the calculated IR spectrum of *Z*-BN which depicts two peaks near 1082 and 1214 cm^{-1}, in agreement with the recorded IR spectra above 22.3 GPa (Fig. 1c).

Electron energy loss spectroscopy (EELS) has been further employed to characterize the valence states of the material. Fig. 4a and b show the EELS spectra for the pristine MWBNNTs and the sample released from 95 GPa, respectively. The N—K edge spectrum related to sp^2 hybridized h-BN shows two separate peaks at 397.8 eV and 403.7 eV which are attributed to transitions of the 1s electrons to π* empty antibonding orbitals and σ* bands, respectively [34,35]. Compared with the pristine MWBNNTs, the σ* peak of the released sample becomes dominating, whereas the π* peak becomes very weak. The decrease of π* peak and the increase of σ* peak is a strong indication of sp^2 to sp^3 conversion in boron nitride materials [35]. The residual π* should be from the surrounding amorphous structures. These results suggest that the released material contains sp^3 hybridized *Z*-BN and a few sp^2 hybridized amorphous components. In addition, we calculated the phonon dispersion curve of Z-BN at 0 GPa to confirm its dynamic stability. As shown in Fig. S1a, no imaginary frequency indicates Z-BN is dynamically stable at ambient pressure and it can be preserved to ambient pressure. We further calculated the relative enthalpies of (15, 15) BNNT and Z-BN. The (15, 15) BNNT was investigated because its inner diameter (~2.03 nm) is similar to that of the sample studied in our experiments. As shown in Fig. S1b, Z-BN is energetically more favorable than (15, 15) BNNT from 0 to 100 GPa, indicating that Z-BN is more stable than (15, 15) BNNT and the spontaneity from (15, 15) BNNT to Z-BN in the transition. Crystal structure parameters for Z-BN were shown in Table S1. Different kinds of nanostructures have different applications [36–39]. Z-BN is a transparent insulator with an indirect band gap of about 5.27 eV, a Vickers hardness of 55.88 GPa and a bulk modulus of 359.61 GPa [14], which make it a potential candidate for advanced electronic devices, coating material, cutting ferrous and carbide-forming hard substances, and so on.

A schematic diagram was plotted to understand the different transformation pathways of h-BN and BNNTs. As shown in Fig. 5a, the nitrogen atoms in the upper layer are coaxial with the boron atoms in the lower layer in h-BN. By applying high pressure, the AA′ stacking is more favorable to the formation of six-membered rings in c-BN and w-BN while the interlayer distance decreases. From topological transition point of view, the various stacking sequences of curved BN layer (described as the B/N atoms face to B/N atoms of neighboring walls) in boron nitride nanotube provide possibilities for 4- and 8-membered BN rings (see Fig. 5b) as curvature increases, which is in contrast to planar h-BN. Note that the even-membered BN rings could hardly be formed in this case due to the highly energetically unfavorable B—B or N—N bonds. This topological consideration suggests that the suitable stacking

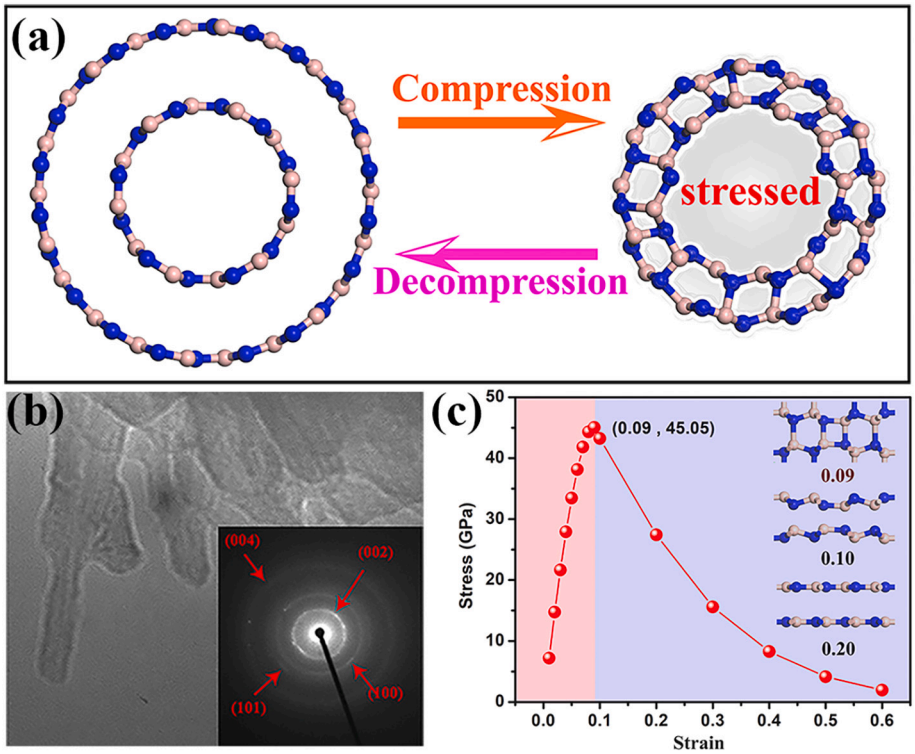

Fig. 6. (a) Cross-section schematic diagram in the pressure cycle of a double-walled boron nitride nanotube. (b) HRTEM image and SAED pattern on the sample released from 45 GPa. (c) Theoretical data for the uniaxial stress plotted as a function of the uniaxial tensile strain along the [010] direction.

sequences in nanotubes can facilitate the creation of new structures. A similar mechanism has also been observed in carbon materials. For instance, Yang et al. proposed V carbon with 5 + 6 + 7 topology by compressing C_{70}@SWNTs peapods, in which the spherical fullerenes lead to different stacking sequences and interactions from graphite [40]. Amsler et al. proposed a possible transition pathway from graphite with only six-membered rings to Z-carbon with four-, six-, and eight-membered rings through simple sliding and buckling of graphene sheets [41].

To understand why the new *Z*-BN can be quenched to ambient conditions, we also study the sample released from lower pressure of 45 GPa. This pressure is sufficient to complete the hBN-to-ZBN phase transition (see Fig. 1). However, our HRTEM observation and selected area electron diffraction (SAED) pattern on the released sample reveal that no *Z*-BN can be detected while the initial tubular geometries with hexagonal structure are almost fully recovered (Fig. 6b). Considering that the *Z*-BN already appeared at above 19.0 GPa, we believe that this fully reversible structure transition should be related to the competition between the resilience of tubes and the stress limitation for the lattice stabilization of *Z*-BN (sp^3 interlinking) upon decompression. As shown in Fig. 6a, when pressure is unloaded, the tube provides radial strength after spring back which gives rise to the cleavage of sp^3 bonds between BN layers. Thus, we carried out first principles approach to investigate the stress-strain curve of our *Z*-BN which is usually used to obtain ultimate fracture tensile stresses of carbon materials and B—N compounds [42–44]. As shown in Fig. 6c, the stress-strain curve shows that the stress increases almost linearly at the initial strains. Then near a strain of 0.09, the stress starts to drop rapidly due to the inter-layered bonds breakdown of Z-BN and the critical strain value is about 45 GPa along [010] direction. Particularly, the resilience of tube was already found to be higher than 45 GPa, leading to the recovery of hexagonal tubular structures (Fig. 6b). Thus, we suggest that Z-BN was unstable and recovered to hexagonal structure with initial tubular geometry when released from 45 GPa. At higher pressure, the tubes distort and collapse and the sp^3-hybridized Z-BN is quenchable to ambient conditions. The results point out that the high resilience of the tube structure becomes a big hindrance to preserving sp^3 bonds upon decompression. Only when the external force exceeds the critical pressure for the nanotube to collapse, the new sp^3 structure can be retained. Besides, it has been reported that the collapse pressure of BNNTs increases with decreasing tube diameter, that is, higher pressure should be applied to break a nanotube with a smaller diameter [45].

Such collapse-induced capture of sp^3 bonded BN structures could also be extended to understand the quenched sp^3 carbon structure from compressing carbon nanotubes. For example, Wang et al. reported that only when the pressure is higher than 75 GPa the formed new superhard carbon phase could be quenched in the experiments of compressing multi-walled carbon nanotubes [46]. Besides, Merlen et al. observed the collapse-induced capture of sp^3-carbon in single-walled carbon nanotubes [47]. They pointed out that the nanotubes with small diameters were good candidates for sp^3 network at high pressure and high temperature conditions. Note that nanotubes usually exhibit extraordinary strength and high resilience, which make them difficult to undergo irreversible collapse upon external forces at room temperature. The high stiffness of nanotubes depends on the diameter/chirality of the tube and the number of walls, which determines the reversibility of nanotubes before complete collapse [48–52]. Efforts have also been made to destruct the tubular structure by using additional shear stresses under pressure [53]. For example, the multiwall carbon nanotubes remain recoverable even after 55 GPa compression, while some irreversible changes by the formation of sp^3 bonding between the tube walls were preserved after tube collapse under pressure with shear [50]. And the irreversible collapse in triple-walled carbon nanotubes was observed at pressures beyond ~60 GPa [54]. Considering a large family of nanotubes, which could be studied as precursors to design new sp^3 hybridized structures by compression, this study provides a possible, general strategy to quench new sp^3 phases to ambient conditions by avoiding elastically radial recovering of transformed nanotubes and thus stabilizing the formed sp^3 structures.

We further hypothesize that the *Z*-BN should be formed firstly by the

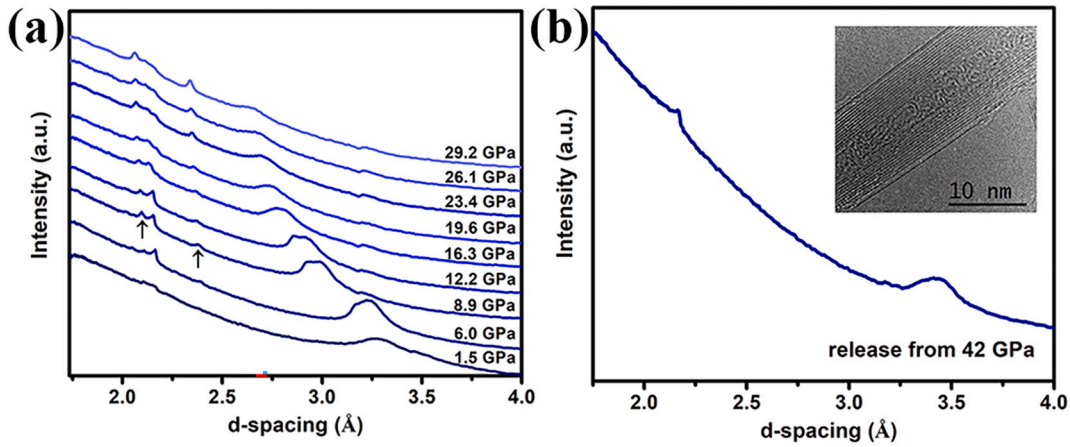

Fig. 7. (a) *In situ* high-pressure XRD patterns of C_{60}-peapods. (b) The XRD pattern of the sample released from 42 GPa. Inset shows the corresponding TEM image.

intertubular/interlayer bonding due to the compression of BN nanotubes. To confirm this conjecture, we designed a comparison experiment by compressing C_{60}@BNNTs and studying the effect of C_{60} filling on the structural transition of BN nanotubes. In this case, the transition into Z-BN occurs at 8.9 GPa (see Fig. 7a), which is much lower than that for the empty BNNTs. This should be due to the additional internal stress from the filled C_{60} molecules inside BN nanotubes during compression which promotes the phase transition. It has been reported that tube filling can enhance collapse pressure of nanotubes and provide larger thermodynamic excursion to obtain sp^3 phases [55,56]. A similar effect has also been observed in fullerene-filled SWNTs [57,58]. In this case, fullerenes with high bulk modulus can be taken as a stiff ball which should generate inhomogeneous stress to the BN nanotube walls. *In situ* high-pressure XRD patterns from compressing C_{60}-peapods also show the appearance of new peaks at d = 2.09 Å and 2.38 Å from *Z*-BN. As pressure increases, Z-BN begins to replace h-BN as the predominant phase in the sample. Like the empty MWBNNTs, the hosting nanotubes were also recovered in the released sample after 42 GPa compression (see Fig. 7b). Note that an irreversible cross-linking between the tube and carbon chains have been proposed when the tube is collapsed under high pressure [59]. The above comparison further shows the intertubular/interlayer bonds of nanotubes cannot be captured before collapsing.

4. Conclusions

A new sp^3 hybridized BN with orthorhombic structure (*Z*-BN) has been successfully synthesized from compressing MWBNNTs with small diameters ranging from 2 to 5 nm. The nested construction composed of coaxial tubes with stronger curvature results in a distinct stacking sequence. Thus, unlike that in compressing hexagonal BN, the MWBNNTs with small diameters are more prone to form new 4- and 8-membered BN rings rather than the 6-membered BN rings observed in cubic or wurtzite structures. Further experiments were carried out to understand the capture mechanism of synthesized Z-BN. It's found that Z-BN started to form above 19 GPa, but was fully recovered to MWBNNTs when released from 45 GPa. Combined with theoretical simulations, we proposed that the irreversible tube collapse is critical for the capture of Z-BN. When released from 93.5 GPa, at which pressure the tubes are fully collapsed, a majority of sp^3 hybridized Z-BN can be obtained. This is owing to the competition between the resilience of tube before collapse and the stress limitation for the lattice stabilization of Z-BN upon decompression. These new findings could shed new light on synthesizing and quenching new structures to ambient conditions and are expected to apply to other tubular materials.

CRediT authorship contribution statement

Ying Zhang: Conceptualization, Methodology, Validation, Investigation, Data curation, Writing-Original draft preparation. **Shuang Liu, Zhen Yao**: Software, Formal analysis. **Jiajun Dong, Bo Liu, Mingrun Du, Peng Wang, Quanjun Li**: Visualization, Investigation. **Thomas Wågberg, Hamid Reza Barzegar, Alex Zettl**: Resources. **Ran Liu, Mingguang Yao, Bingbing Liu**: Writing-Reviewing and Editing, Funding acquisition.

Declaration of competing interest

The authors declare that they have no known competing financial interests or personal relationships that could have appeared to influence the work reported in this paper.

Data availability

Data will be made available on request.

Acknowledgments

This work was supported financially by the National Key Research and Development Program of China (2018YFA0305900, 2018YFA0703404), the National Natural Science Foundation of China (52225203, 51822204, 51320105007, 11634004, 12104175). BNNT synthesis was supported by the U.S. Department of Energy, Office of Science, Office of Basic Energy Sciences, Materials Sciences and Engineering Division, under Contract No. DE-AC02-05-CH11231 within the sp^2-Bonded Materials Program (KC2207).

Appendix A. Supplementary data

Supplementary data to this article can be found online at https://doi.org/10.1016/j.diamond.2022.109431.

References

[1] T. Irifune, A. Kurio, S. Sakamoto, T. Inoue, H. Sumiya, Ultrahard polycrystalline diamond from graphite, Nature 421 (6923) (2003) 599–600.
[2] R.B. Kaner, J.J. Gilman, S.H. Tolbert, Designing superhard materials, Science 308 (5726) (2005) 1268–1269.
[3] P.F. McMillan, New materials from high-pressure experiments, Nat. Mater. 1 (1) (2002) 19–25.
[4] Y. Tian, B. Xu, D. Yu, Y. Ma, Y. Wang, Y. Jiang, W. Hu, C. Tang, Y. Gao, K. Luo, Z. Zhao, L.M. Wang, B. Wen, J. He, Z. Liu, Ultrahard nanotwinned cubic boron nitride, Nature 493 (7432) (2013) 385–388.

[5] K.D. Timmerhaus, High-Pressure Science and Technology: Volume 1: Physical Properties and Material Synthesis/Volume 2: Applications and Mechanical Properties, Springer Science & Business Media, 2013.
[6] R.H. Wentorf, R.C. DeVries, F.P. Bundy, Sintered superhard materials, Science 208 (4446) (1980) 873–880.
[7] M. Keunecke, E. Wiemann, K. Weigel, S.T. Park, K. Bewilogua, Thick c-BN coatings – preparation, properties and application tests, Thin Solid Films 515 (3) (2006) 967–972.
[8] V.L. Solozhenko, O.O. Kurakevych, Y. Le Godec, Creation of nanostuctures by extreme conditions: high-pressure synthesis of ultrahard nanocrystalline cubic boron nitride, Adv. Mater. 24 (12) (2012) 1540–1544.
[9] M. Xiong, C. Fan, Z. Zhao, Q. Wang, J. He, D. Yu, Z. Liu, B. Xu, Y. Tian, Novel three-dimensional boron nitride allotropes from compressed nanotube bundles, J. Mater. Chem. C 2 (34) (2014) 7022–7028.
[10] X. Yang, S. Zhou, S. Huang, J. Zhao, New boron nitride monolith phases from high-pressure compression of double-walled boron nitride nanotubes, J. Chem. Phys. 154 (13) (2021), 134702.
[11] M. Xiong, K. Luo, D. Yu, Z. Zhao, J. He, G. Gao, Pressure-induced boron nitride nanotube derivatives: 3D metastable allotropes, J. Appl. Phys. 121 (16) (2017), 165106.
[12] B. Wen, J. Zhao, R. Melnik, Y. Tian, Body-centered tetragonal B2N2: a novel sp3 bonding boron nitride polymorph, Phys. Chem. Chem. Phys. 13 (32) (2011) 14565–14570.
[13] R. Zhou, J. Dai, X. Cheng Zeng, Structural, electronic and mechanical properties of sp(3)-hybridized BN phases, Phys. Chem. Chem. Phys. 19 (15) (2017) 9923–9933.
[14] C. He, L. Sun, C. Zhang, X. Peng, K. Zhang, J. Zhong, Z-BN: a novel superhard boron nitride phase, Phys. Chem. Chem. Phys. 14 (31) (2012) 10967–10971.
[15] S. Nakano, O. Fukunaga, New scope of high pressure-high temperature synthesis of cubic boron nitride, Diam. Relat. Mater. 2 (11) (1993) 1409–1413.
[16] A. Onodera, K. Inoue, H. Yoshihara, H. Nakae, T. Matsuda, T. Hirai, Synthesis of cubic boron nitride from rhombohedral form under high static pressure, J. Mater. Sci. 25 (10) (1990) 4279–4284.
[17] Z. Dong, Y. Song, Transformations of cold-compressed multiwalled boron nitride nanotubes probed by infrared spectroscopy, J. Phys. Chem. C 114 (4) (2010) 1782–1788.
[18] C. Chen, D. Yin, T. Kato, T. Taniguchi, K. Watanabe, X. Ma, H. Ye, Y. Ikuhara, Stabilizing the metastable superhard material wurtzite boron nitride by three-dimensional networks of planar defects, Proc. Natl. Acad. Sci. U. S. A. 116 (23) (2019) 11181–11186.
[19] Y. Meng, H.K. Mao, P.J. Eng, T.P. Trainor, M. Newville, M.Y. Hu, C. Kao, J. Shu, D. Hausermann, R.J. Hemley, The formation of sp3 bonding in compressed BN, Nat. Mater. 3 (2) (2004) 111–114.
[20] S. Saha, V. Gadagkar, P.K. Maiti, D.V.S. Muthu, D. Golberg, C. Tang, C. Zhi, Y. Bando, A.K. Sood, Irreversible pressure-induced transformation of boron nitride nanotubes, J. Nanosci. Nanotechnol. 7 (6) (2007) 1810–1814.
[21] J.Y. Huang, Y.T. Zhu, Atomic-scale structural investigations on the nucleation of cubic boron nitride from amorphous boron nitride under high pressures and temperatures, Chem. Mater. 14 (4) (2002) 1873–1878.
[22] T. Taniguchi, K. Kimoto, M. Tansho, S. Horiuchi, S. Yamaoka, Phase transformation of amorphous boron nitride under high pressure, Chem. Mater. 15 (14) (2003) 2744–2751.
[23] T. Sato, T. Ishii, N. Setaka, Formation of cubic boron nitride from rhombohedral boron nitride by explosive shock compression, Journal of the American Ceramic Society 65 (10) (1982) c162-c162.
[24] R. Cuscó, J. Pellicer-Porres, J.H. Edgar, J. Li, A. Segura, L. Artús, Pressure dependence of the interlayer and intralayer E2g raman-active modes of hexagonal BN up to the wurtzite phase transition, Phys. Rev. B 102 (7) (2020), 075206.
[25] X. Zhang, Y. Wang, J. Lv, C. Zhu, Q. Li, M. Zhang, Q. Li, Y. Ma, First-principles structural design of superhard materials, J. Chem. Phys. 138 (11) (2013), 114101.
[26] S. Xu, L. Wang, X. Qiao, X. Xu, Y. Cai, Novel BN polymorphs transformed from the smallest BNNTs under high pressure, Comput. Mater. Sci. 110 (2015) 241–246.
[27] S.D. Silva-Santos, A. Impellizzeri, A.L. Aguiar, C. Journet, C. Dalverny, B. Toury, J. M. De Sousa, C.P. Ewels, A. San-Miguel, High pressure in boron nitride nanotubes for kirigami nanoribbon elaboration, J. Phys. Chem. C 125 (21) (2021) 11440–11453.
[28] A. Fathalizadeh, T. Pham, W. Mickelson, A. Zettl, Scaled synthesis of boron nitride nanotubes, nanoribbons, and nanococoons using direct feedstock injection into an extended-pressure, inductively-coupled thermal plasma, Nano Lett. 14 (8) (2014) 4881–4886.
[29] T. Pham, A. Fathalizadeh, B. Shevitski, S. Turner, S. Aloni, A. Zettl, A universal wet-chemistry route to metal filling of boron nitride nanotubes, Nano Lett. 16 (1) (2016) 320–325.
[30] D.V.S. Muthu, A.E. Midgley, E.A. Petruska, A.K. Sood, Y. Bando, D. Golberg, M. B. Kruger, High-pressure effects on boron nitride multi-walled nanotubes: an X-ray diffraction study, Chem. Phys. Lett. 466 (4–6) (2008) 205–208.
[31] C. Ji, V.I. Levitas, H. Zhu, J. Chaudhuri, A. Marathe, Y. Ma, Shear-induced phase transition of nanocrystalline hexagonal boron nitride to wurtzitic structure at room temperature and lower pressure, Proc. Natl. Acad. Sci. U. S. A. 109 (47) (2012) 19108–19112.
[32] E. Borowiak-Palen, T. Pichler, G.G. Fuentes, B. Bendjemil, X. Liu, A. Graff, G. Behr, R.J. Kalenczuk, M. Knupfer, J. Fink, Infrared response of multiwalled boron nitride nanotubes, Chem Commun (Camb) 1 (2003) 82–83.
[33] A. Segura, R. Cuscó, T. Taniguchi, K. Watanabe, G. Cassabois, B. Gil, L. Artús, High-pressure softening of the out-of-plane A2u(transverse-optic) mode of hexagonal boron nitride induced by dynamical buckling, J. Phys. Chem. C 123 (28) (2019) 17491–17497.
[34] H.K. Schmid, Phase identification in carbon and BN systems by EELS, Microsc. Microanal. Microstruct. 6 (1) (1995) 99–111.
[35] M. Jaouen, G. Hug, V. Gonnet, G. Demazeau, G. Tourillon, An EELS and XAS study of cubic boron nitride synthesized under high pressure - high temperature conditions, Microsc. Microanal. Microstruct. 6 (1) (1995) 127–139.
[36] M.C. Han, H.W. He, W.K. Kong, K. Dong, B.Y. Wang, X. Yan, L.M. Wang, X. Ning, High-performance electret and antibacterial polypropylene meltblown nonwoven materials doped with boehmite and ZnO nanoparticles for air filtration, Fibers Polym. 23 (7) (2022) 1947–1955.
[37] Y. Zhang, Z. Pan, J. Yang, J. Chen, K. Chen, K. Yan, X. Meng, X. Zhang, M. He, Study on the suppression mechanism of (NH4)2CO3 and SiC for polyethylene deflagration based on flame propagation and experimental analysis, Powder Technol. 399 (2022), 117193.
[38] X. Zhang, Y. Tang, F. Zhang, C.S. Lee, A novel aluminum-graphite dual-ion battery, Adv. Energy Mater. 6 (11) (2016) 1502588.
[39] X. Fan, G. Wei, X. Lin, X. Wang, Z. Si, X. Zhang, Q. Shao, S. Mangin, E. Fullerton, L. Jiang, W. Zhao, Reversible switching of interlayer exchange coupling through atomically thin VO2 via electronic state modulation, Matter 2 (6) (2020) 1582–1593.
[40] X. Yang, M. Yao, X. Wu, S. Liu, S. Chen, K. Yang, R. Liu, T. Cui, B. Sundqvist, B. Liu, Novel superhard sp^{3} carbon allotrope from cold-compressed C_{70} peapods, Phys. Rev. Lett. 118 (24) (2017), 245701.
[41] M. Amsler, J.A. Flores-Livas, L. Lehtovaara, F. Balima, S.A. Ghasemi, D. Machon, S. Pailhes, A. Willand, D. Caliste, S. Botti, A. San Miguel, S. Goedecker, M. A. Marques, Crystal structure of cold compressed graphite, Phys. Rev. Lett. 108 (6) (2012), 065501.
[42] B.A. Fairchild, S. Rubanov, D.W. Lau, M. Robinson, I. Suarez-Martinez, N. Marks, A.D. Greentree, D. McCulloch, S. Prawer, Mechanism for the amorphisation of diamond, Adv. Mater. 24 (15) (2012) 2024–2029.
[43] Y. Li, J. Hao, H. Liu, S. Lu, J.S. Tse, High-energy density and superhard nitrogen-rich B-N compounds, Phys. Rev. Lett. 115 (10) (2015), 105502.
[44] R.H. Telling, C.J. Pickard, M.C. Payne, J.E. Field, Theoretical strength and cleavage of diamond, Phys. Rev. Lett. 84 (22) (2000) 5160.
[45] S.S. Coutinho, V. Lemos, S. Guerini, Band-gap tunability of a (6,0) BN nanotube bundle under pressure: ab initiocalculations, Phys. Rev. B 80 (19) (2009), 193408.
[46] Z. Wang, Y. Zhao, K. Tait, X. Liao, D. Schiferl, C. Zha, R.T. Downs, J. Qian, Y. Zhu, T. Shen, A quenchable superhard carbon phase synthesized by cold compression of carbon nanotubes, Proc. Natl. Acad. Sci. 101 (38) (2004) 13699–13702.
[47] A. Merlen, P. Toulemonde, S.Le Floch, G. Montagnac, T. Hammouda, O. Marty, A. San Miguel, High pressure–high temperature synthesis of diamond from single-wall pristine and iodine doped carbon nanotube bundles, Carbon 47 (7) (2009) 1643–1651.
[48] X. Wei, M.S. Wang, Y. Bando, D. Golberg, Tensile tests on individual multi-walled boron nitride nanotubes, Adv. Mater. 22 (43) (2010) 4895–4899.
[49] J. Garel, I. Leven, C. Zhi, K.S. Nagapriya, R. Popovitz-Biro, D. Golberg, Y. Bando, O. Hod, E. Joselevich, Ultrahigh torsional stiffness and strength of boron nitride nanotubes, Nano Lett. 12 (12) (2012) 6347–6352.
[50] E.Y. Pashkin, A.M. Pankov, B.A. Kulnitskiy, I.A. Perezhogin, A.R. Karaeva, V. Z. Mordkovich, M.Y. Popov, P.B. Sorokin, V.D. Blank, The unexpected stability of multiwall nanotubes under high pressure and shear deformation, Appl. Phys. Lett. 109 (8) (2016), 081904.
[51] Y. Magnin, F. Rondepierre, W. Cui, D.J. Dunstan, A. San-Miguel, Collapse phase diagram of carbon nanotubes with arbitrary number of wallsCollapse modes and macroscopic analog, Carbon 178 (2021) 552–562.
[52] A.C. Torres-Dias, S. Cambré, W. Wenseleers, D. Machon, A. San-Miguel, Chirality-dependent mechanical response of empty and water-filled single-wall carbon nanotubes at high pressure, Carbon 95 (2015) 442–451.
[53] V.D. Blank, V.N. Denisov, A.N. Kirichenko, N.A. Lvova, S.Y. Martyushov, B. N. Mavrin, D.M. Popova, M.Y. Popov, E.V. Tat'yanin, A.A. Zakhidov, Nanostructured superhard carbon phase obtained under high pressure with shear deformation from single-wall nanotubes HiPco, Physica B: Condensed Matter 382 (1-2) (2006) 58–64.
[54] S.D. Silva-Santos, R.S. Alencar, A.L. Aguiar, Y.A. Kim, H. Muramatsu, M. Endo, N. P. Blanchard, A. San-Miguel, A.G. Souza Filho, From high pressure radial collapse to graphene ribbon formation in triple-wall carbon nanotubes, Carbon 141 (2019) 568–579.
[55] C. Bousige, A. Stolz, S.D. Silva-Santos, J. Shi, W. Cui, C. Nie, M.A.L. Marques, E. Flahaut, M. Monthioux, A. San-Miguel, Superior carbon nanotube stability by molecular filling:a single-chirality study at extreme pressures, Carbon 183 (2021) 884–892.
[56] D. Machon, V. Pischedda, S. Le Floch, A. San-Miguel, Perspective: high pressure transformations in nanomaterials and opportunities in material design, J. Appl. Phys. 124 (16) (2018), 160902.
[57] C. Caillier, D. Machon, A. San-Miguel, R. Arenal, G. Montagnac, H. Cardon, M. Kalbac, M. Zukalova, L. Kavan, Probing high-pressure properties of single-wall carbon nanotubes through fullerene encapsulation, Phys. Rev. B 77 (12) (2008), 125418.
[58] B. Anis, F. Börrnert, M.H. Rümmeli, C.A. Kuntscher, High-pressure optical microspectroscopy study on single-walled carbon nanotubes encapsulating C60, J. Phys. Chem. C 117 (42) (2013) 21995–22001.
[59] W.Q. Neves, R.S. Alencar, R.S. Ferreira, A.C. Torres-Dias, N.F. Andrade, A. San-Miguel, Y.A. Kim, M. Endo, D.W. Kim, H. Muramatsu, A.L. Aguiar, A.G. Souza Filho, Effects of pressure on the structural and electronic properties of linear carbon chains encapsulated in double wall carbon nanotubes, Carbon 133 (2018) 446–456.

Supporting Information

Capture of novel *sp*^{3} hybridized Z-BN by compressing boron nitride nanotubes with small diameter

Ying Zhang,[a] Shuang Liu,[a] Zhen Yao,[a] Jiajun Dong,[a] Bo Liu,[a] Ran Liu,[a,*] Mingrun Du,[b] Peng Wang,[a] Quanjun Li,[a] Thomas Wågberg,[c] Hamid Reza Barzegar,[c] Alex Zettl,[d] Mingguang Yao,[a,*] and Bingbing Liu[a,*]

[a] State Key Laboratory of Superhard Materials, College of Physics, Jilin University, Changchun 130012, China

[b] Civil Aviation University of China, College of Science, Tianjin 300300, China

[c] Department of Physics, Umeå University, 90187 Umeå, Sweden

[d] Department of Physics, University of California at Berkeley,
Materials Sciences Division, Lawrence Berkeley National Laboratory,
Kavli Energy Nano Science Institute at the University of California at Berkeley,
Lawrence Berkeley National Laboratory, Berkeley, California, 94720, USA

* Corresponding author

E-mail addresses:

liuran@jlu.edu.cn (R. Liu), yaomg@jlu.edu.cn (M. Yao), liubb@jlu.edu.cn (B. Liu).

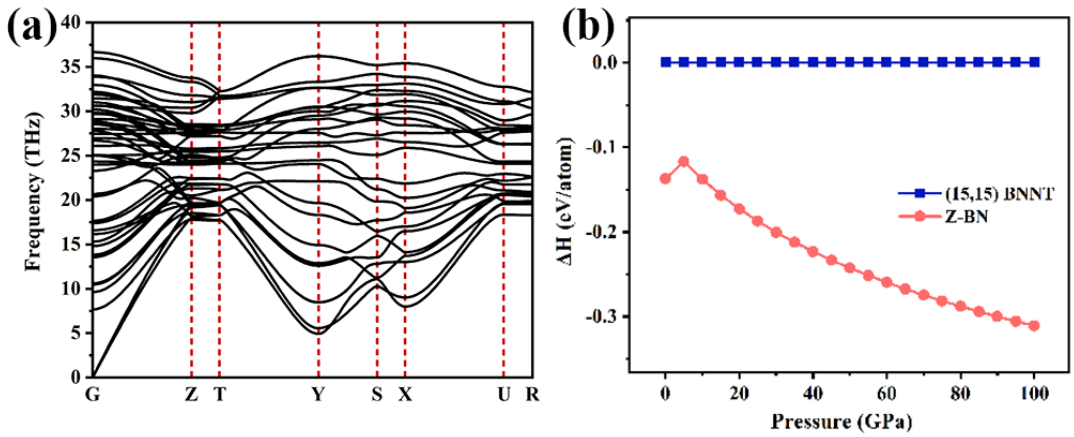

Figure.S1. (a) The phonon dispersion curves for Z-BN at 0 GPa. (b) Enthalpy-pressure diagrams of (15,15) BNNTs and Z-BN.

Table S1. Crystal structure parameters for Z-BN.

	Space Group	**Lattice Parameters**	**Wyckoff Positions**			
Z-BN	*Pbam*	a = 8.89 Å, b = 4.29 Å, c = 2.55 Å	B1	0.334	0.827	0.000
		α = β = γ = 90°	B2	0.088	0.827	0.500
			N1	0.834	0.301	0.000
			N2	0.589	0.301	0.500